



## Climate variability in a simple model of warm climate land-atmosphere interaction

Jiangfeng Wei,<sup>1</sup> Robert E. Dickinson,<sup>1</sup> and Ning Zeng<sup>2</sup>

Received 29 August 2005; revised 4 April 2006; accepted 27 April 2006; published 18 August 2006.

[1] A simple model is developed to describe the significant land-atmosphere interaction processes in the warm climate. It includes bulk soil hydrology, dynamic vegetation, and simple land-atmosphere interaction processes. The model can simulate the basic features of land surface control on evapotranspiration (ET) and exhibits a multiequilibrium behavior similar to that of some more complex models. In order to study the role of land surface processes in climate variability on monthly to seasonal timescales, a series of experiments are performed with the model over different land covers and at different external forcings. The major findings are: (1) The maximum soil wetness memory and precipitation predictability tend to occur at a sparser (denser) vegetation cover with the weakening (strengthening) of external forcing. (2) For vegetated region, the soil moisture memory and precipitation persistence will be underestimated if vegetation is not interactive, and the percentage of underestimation is larger over denser vegetation covers. (3) Interactive vegetation can enhance the low-frequency coherency between soil wetness and precipitation, but its influence on high-frequency coherency is small. (4) Large coherencies between soil wetness and precipitation in the time-frequency domain correspond to strong wavelet power of external forcing in the same domain. These findings provide guidance for the development of and study with more complex models.

**Citation:** Wei, J., R. E. Dickinson, and N. Zeng (2006), Climate variability in a simple model of warm climate land-atmosphere interaction, *J. Geophys. Res.*, *111*, G03009, doi:10.1029/2005JG000096.

### 1. Introduction

[2] Land-atmosphere interaction includes complex feedbacks among soil, vegetation, and atmosphere [e.g., *Rodriguez-Iturbe et al.*, 1999a], and the understanding of it is hindered by the heterogeneity of land surface properties and the chaotic nature of the atmosphere. All kinds of efforts (e.g., remote sensing, field experiments) are made to study these processes. Currently, modeling is still a primary approach due to limited observations, especially for long-timescale and large-space-scale processes.

[3] Land surface models have advanced from a bucket-type parameterization in the 1960s to the current soil-vegetation-atmosphere interactive schemes with carbon and nitrogen cycle (see *Pitman* [2003] for a review). However, intercomparison shows that different land models, even with the same atmospheric forcing, still give significantly different surface fluxes and soil wetness [*Henderson-Sellers et al.*, 1995]. These differences come from the different parameterizations of individual processes and the amplification of the differences by the nonlinearity of the models. Complex models include detailed description of

various processes, but the useful signals are often drowned out by all kinds of noise. These complex models are not always suitable for mechanistic study, so various simple models have been developed and are proven to be efficient for some purposes [e.g., *Rodriguez-Iturbe et al.*, 1991; *Zeng*, 1998; *Liu and Avissar*, 1999; *Zeng et al.*, 2004]. As noise in real climate system or GCMs (general circulation models) may distort some of the relationships or even make them indiscernible, simple models which properly describe the important processes and have much less noise can be more easily used to find such relationships. Current climate models are not only complex but also computationally expensive, and most simulations are performed without a hypothesis as to the expected results, so simulations often have to be done several times to select the best experimental design. Such repetition can be very time and energy consuming for studying longer periods. It is thus preferable to obtain some qualitative results to guide the long-term integration of GCMs.

[4] The impact of land cover change on climate has been a concern since the 1970s [e.g., *Charney*, 1975]. Many modeling studies have been done on the mean climate change caused by land cover changes in the African Sahel [e.g., *Xue and Shukla*, 1993; *Zheng and Eltahir*, 1997; *Clark et al.*, 2001; *Taylor et al.*, 2002], the Amazon [e.g., *Dickinson and Henderson-Sellers*, 1988; *Lean and Warrilow*, 1989; *Dickinson and Kennedy*, 1992], and other regions [e.g., *Xue*, 1996; *Fu*, 2003]. Land cover change can

<sup>1</sup>School of Earth and Atmospheric Sciences, Georgia Institute of Technology, Atlanta, Georgia, USA.

<sup>2</sup>Department of Atmospheric and Oceanic Science and Earth System Science, Interdisciplinary Center, University of Maryland at College Park, College Park, Maryland, USA.

impact not only the mean climate but also the climate variability [Voldoire and Royer, 2004], and the extreme climate (e.g., drought and flood) may be more important for us than the mean climate. Hence we will focus on climate variability in this study.

[5] Soil and vegetation are two main components of land surface, and they are the primary site for the exchange of water, energy, and momentum between land and atmosphere. As soil moisture and vegetation change have memories considerably longer than most of the atmospheric processes, coupling them to the atmosphere can contribute to the skills of climate simulation from seasonal [Delworth and Manabe, 1989; Koster and Suarez, 1995; Koster et al., 2000, 2004; Xue et al., 2004; Levis and Bonan, 2004] to decadal timescales [Zeng et al., 1999; Wang and Eltahir, 2000a; Wang et al., 2004; Delire et al., 2004; Brovkin et al., 2003]. Because of the limitations of computational resources and models, simulations with coupled GCM-DGVMs (dynamic global vegetation model) are still not very common. Most current studies of land-atmosphere interaction focus on the feedback between soil moisture and precipitation, and the vegetation is fixed at seasonal climatologies. However, in reality the vegetation will change with climate and has some memory, so it will not immediately recover after a drought or a long dry season. A main purpose of this study is to reveal how the interactive vegetation influences land-atmosphere interaction and the simulated climate variability, especially the coupling of soil moisture and precipitation.

[6] We assumed that the region studied is warm enough throughout the year, so temperature is not a stress for ET and vegetation growth, and most precipitation is convective (e.g., tropical land). On the basis of this assumption, a simple model of warm climate land-atmosphere interaction is developed. It includes land surface processes important for long-term land-atmosphere interaction, and an empirical relation between precipitation and other variables. The model is then used to study the role of interactive soil moisture and vegetation in climate variability and predictability. Monthly to seasonal timescale process is the focus of this paper. Section 2 describes the model in detail; section 3 gives the performance and behavior of the model; section 4 presents the experiments and results. Conclusions and discussion are given in section 5.

## 2. Model Description

[7] A one-dimensional model is developed to simulate the major physical and biophysical processes in warm climate land-atmosphere interaction. It includes bulk soil hydrology, dynamic vegetation, and land-atmosphere interaction processes: ET and precipitation. The model simulates the land surface fluxes at large spatial and long temporal scales by statistically taking into account smaller and faster scale variations, so it is suitable for monthly to decadal scale study. It is not intended to give a precise description of all kind of processes, but to focus on their interaction and hence study the role of these processes in climate variability.

### 2.1. Evapotranspiration

[8] It is assumed that the vegetated area and bare ground are evenly distributed and they have the same soil moisture

after spatial interaction. ET is described here using a set of simplified formulas. Evaporation from the bare ground is calculated as

$$E_b = E_p \eta(S), \quad (1)$$

where  $E_p$  is potential ET,  $\eta$  is water stress for evaporation over ground ( $0 \leq \eta \leq 1$ ) [Dingman, 2002], and  $S$  ( $0 \leq S \leq 1$ ) is soil wetness (ratio of volumetric soil water content to soil porosity). We assumed that under the land surface change, the change in ET due to soil wetness and vegetation changes dominates over other effects such as wind and humidity changes, so  $E_p$  is given as a constant.  $\eta$  is a function of soil moisture and soil properties. If soil properties do not change, it is only a function of soil moisture

$$\eta(S) = [(S - S_{wp}) / (S_{fc} - S_{wp})]^c, \quad (2)$$

where  $S_{wp}$  is soil wilting point, and  $S_{fc}$  is field capacity. When  $S < S_{wp}$ ,  $\eta = 0$ . The exponent  $c$  accounts for the possible nonlinear dependence of evaporation on water deficit.

[9] Vegetation shading is accounted for by taking the soil evaporation under the vegetation as

$$E_v = E_p \eta(S) e^{-k_b L}, \quad (3)$$

where  $L$  is leaf area index (LAI), and  $k_b$  is the canopy extinction coefficient that controls what fraction of the soil surface beneath a canopy is directly exposed to the atmosphere above the canopy [Campbell and Norman, 1998]. As the interception and transpiration may compensate each other with almost no change in the total [Wang and Eltahir, 2000b], and their effects on soil moisture are also the same, transpiration and interception losses are lumped as

$$TI = E_p \beta(S) (1 - e^{-k_b L}), \quad (4)$$

where  $\beta(S)$  is vegetation water stress and is defined as

$$\beta(S) = \left[ \frac{\left( S - S_{wp} \left( 1 - \frac{L_w}{L_x} \right) \right)}{\left( S_{fc} - S_{wp} \left( 1 - \frac{L_w}{L_x} \right) \right)} \right]^q. \quad (5)$$

This expression is similar to evaporation water stress in (2) but accounts for water uptake by roots from deep layers by decreasing total  $S_{wp}$  with increasing rooting depth, and the rooting depth is assumed to be proportional to  $L_w$  (see section 2.3 for  $L_w$  and  $L_x$ ). Exponent  $q$  accounts for the nonlinear dependence of vegetation water stress on soil saturation in the bulk model [Rodriguez-Iturbe et al., 1999b].

[10] The fraction of vegetation coverage is approximated as

$$f = L/L_x, \quad (6)$$

where  $L_x$  is the maximum LAI given as 6. The total ET from this area, including vegetated and bare land, is

$$ET = f(E_v + TI) + (1 - f)E_b. \quad (7)$$

## 2.2. Soil Hydrology

[11] The water budget equation for a single soil layer is

$$D\phi \frac{\partial S}{\partial t} = P - ET - R, \quad (8)$$

where  $D$  is the depth of hydrologically active soil,  $\phi$  is soil porosity, and  $P$  is precipitation. Runoff  $R$  includes surface runoff  $R_s$  and subsoil gravitational drainage  $R_d$ , and is parameterized simply as [e.g., Dickinson *et al.*, 1993]

$$R_s = (P - ET)S^4 \quad (9)$$

$$R_d = K_s S^{2B+3}, \quad (10)$$

where  $K_s$  is saturated hydraulic conductivity, and  $B$  is the Clapp-Hornberger exponent [Clapp and Hornberger, 1978].

## 2.3. Vegetation Dynamics

[12] The simple dynamic vegetation model is based on the simple LAI model of Zeng *et al.* [1999], but adds a seasonal time dependence to model the seasonal variation of vegetation (leaf phenology). This model considers the dependence of photosynthesis on soil moisture by retaining the major biophysical aspects of some complex dynamic vegetation models [e.g., Foley *et al.*, 1996; Cramer *et al.*, 2001], but sidesteps the carbon cycle completely. It predicts LAI  $L$  once a day as

$$\frac{\partial L}{\partial t} = a\beta(S)(1 - e^{-k_p L}) - \frac{L}{\tau_l}, \quad (11)$$

and predicts potential maximum LAI  $L_w$  annually as

$$\frac{\partial L_w}{\partial t} = b\beta(S)(1 - e^{-k_p L_w}) - \frac{L_w}{\tau_w}. \quad (12)$$

$L$ ,  $L_w > 0$ . The first terms on the rhs of equations (11) and (12) represent photosynthesis while the second terms represent vegetation losses. Their parameters are:  $k_p$ , the extinction coefficient of photosynthetically active radiation,  $\tau_l$ , the leaf growth (phenology) timescale,  $\tau_w$ , the timescale of vegetation type transition (succession), and  $L_w$ , the maximum leaf area that currently can be supported. Both  $\tau_l$  and  $\tau_w$  depend on climate, vegetation and soil properties.  $L_w$  is associated with vegetation types, and trees have larger  $L_w$  than grasses because they can support more leaves. For a certain area,  $L$  can never exceed  $L_w$ .  $L_w$  is not related to current LAI and is only related to climate condition and vegetation types. The coefficients  $a$ ,  $b$  are chosen such that under optimal

climate conditions ( $\beta = 1$ ), vegetation would grow to its maximum LAI ( $L = L_w$ ,  $L_w = L_x$ ), so

$$a = \frac{L_w}{\tau_l(1 - e^{-k_p L_w})} \quad (13)$$

$$b = \frac{L_x}{\tau_w(1 - e^{-k_p L_x})}. \quad (14)$$

[13] Although the vegetation model only describes the natural growth of vegetation, the influence of human activities can be added by prescribing some variables. For example, a sudden deforestation can be included by taking  $L_w = 0.01$  (this is the prescribed minimum LAI to make vegetation able to start again in the model), and  $L_w$  and  $L$  can be given values to represent planting. The initial value of  $L_w$  depends on the vegetation type planted, and saplings should have larger  $L_w$  than seeds.

## 2.4. Precipitation

[14] Precipitation has much uncertainty due to its large temporal and spatial variabilities. In order to decrease these uncertainties, we assumed that the spatial scale we are modeling is regional to continental scale. The precipitable water comes from local ET and horizontal transport, so the precipitation is calculated as

$$P = ET \cdot PE/\rho + \sigma \cdot F(t), \quad (15)$$

where  $PE$  is precipitation efficiency (PE),  $\rho$  is water recycling ratio,  $F$  is added external forcing, and  $\sigma$  is its forcing strength. PE is the fraction of input moisture flux that falls as precipitation, and it is associated with both local and large-scale factors [Eltahir and Bras, 1996]. We express it as

$$PE = PE_{\min} + \alpha[f(1 - e^{-mL}) + (1 - f)S], \quad (16)$$

where  $PE_{\min}$  is the minimum PE when the land is very dry and has no vegetation,  $\alpha$  is the strength of vegetation and soil wetness to trigger and sustain precipitation through the influence of albedo and roughness length [Lofgren, 1995; Eltahir, 1996, 1998], and  $m$  is an empirical coefficient. This expression qualitatively considers local impact of vegetation and soil moisture on rainfall.

[15] The water recycling ratio  $\rho$  is defined as the ratio of moisture from local ET versus the total of local ET and horizontal transport [Trenberth, 1999]. It is influenced by both local and surrounding thermal changes and has a seasonal cycle [Brubaker *et al.*, 1993]. It is assumed sinusoidal as

$$\rho = \bar{\rho} + \sigma_\rho \sin(2\pi t/T). \quad (17)$$

Although other model variables, such as potential ET, temperature stress, and PE, could also have a seasonal cycle like  $\rho$ , such are not considered here to maintain simplicity. The constant recycling ratio assumes a linear relationship between ET and horizontal moisture transport. Such is expected in a deep convective region where a small perturbation to local energy balance will cause a large-

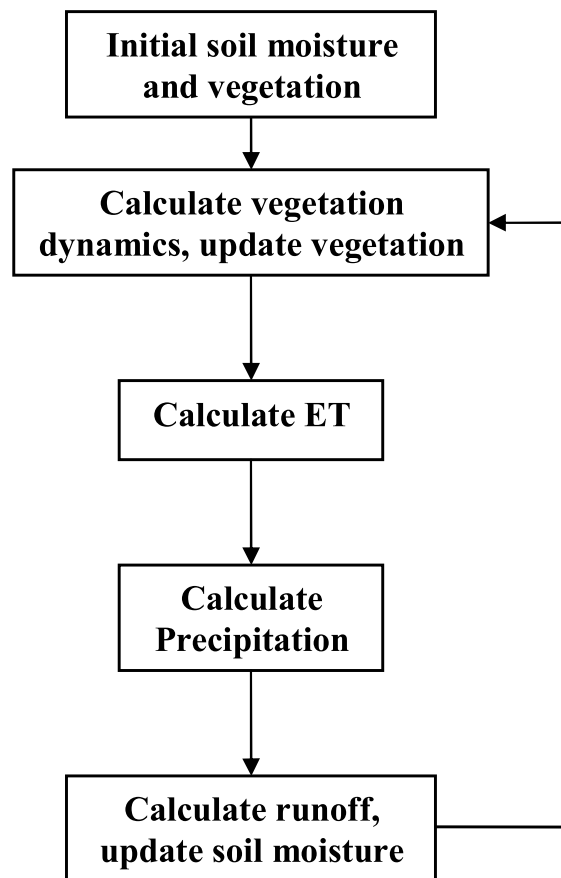


Figure 1. Schematic of the model integration cycle.

scale atmospheric circulation change such that moisture convergence feedback is quasi-linearly proportional to change in local moisture static energy which includes ET [Zeng and Neelin, 1999]. Most warm climate rainfall is deep convective.

[16] The last term of (15) is a random time series to describe the uncertainty of precipitation due to the nonlocal variability, such as that from SST variation and ENSO, and the internal variability from atmospheric dynamics. Hereafter, these two variabilities are together referred to as the “external forcing” because they are not from the local land-atmosphere interaction processes described here.  $F$  is given as a white noise added onto a red noise to represent different processes and forcings in the atmosphere ( $F$  has a mean of 0 and a standard deviation of 1.57 here). In fact, the last term lumps the disturbances of  $ET$ ,  $PE$  and  $\rho$ . Although such external forcing could influence almost every part of the land-atmosphere interaction, it is only added to precipitation to keep the simulation simple and aid the physical interpretation of the results.

## 2.5. Model Implementation

[17] The sequence of model calculations is shown in Figure 1. Initial soil moistures and vegetation are needed to start the integration. A forward difference scheme is used to integrate the differential equations. Unless otherwise mentioned, the parameter values used in the model are shown in Table 1. They are some characteristic values for the tropics and not for a specific area. The time step for the

integrations is 1 day, and equation (12) is integrated once a year. For simplicity, each month is 30 days and each year is 360 days. Considering the coarse parameterization of the model, only monthly mean values of the outputs are used for analysis.

## 3. Model Performance and Behavior

[18] The model-simulated mean annual cycle of soil wetness, precipitation, LAI, and ET are shown in Figure 2. LAI lags precipitation and soil wetness, which is consistent with observations [Zhang *et al.*, 2005], and the exact time of lag depends on vegetation types ( $L_w$ ) and leaf phenology ( $\tau_l$ ). Figure 3 shows the ET over its potential value as a function of soil saturation for fully vegetated and bare land. Their relationships are nonlinear. Vegetated land has larger ET for the same soil wetness because vegetation can take up water from deep layers, hence making the deep soil drier [Scanlon *et al.*, 2005]. If soil wetness is larger than or equal to field capacity, ET is equal to its potential value. The results are consistent with those of Lowry [1959] (also referred to by Rodriguez-Iturbe *et al.* [1991]). They demonstrate the model’s ability to capture the basic features of land surface control on ET.

[19] Many studies have demonstrated that a water-constrained biosphere-atmosphere system can have multiple equilibrium states at a certain parameter regime [Zeng and Neelin, 2000; Wang, 2004; Zeng *et al.*, 2004; Liu *et al.*, 2005; D’Odorico *et al.*, 2005], and our model also shows such a feature. This can be illustrated clearly in Figure 4. As this is a coupled model, the change of climate states (dry or wet) can be realized by changing some model parameters, such as the parameters in the formation of precipitation efficiency and recycling ratio (equations (15) and (16)). Figure 4 shows how the equilibrium states of the system are determined by  $PE_{\min}$ ,  $\alpha$ , and  $\rho$ . The parameter space is divided into three regimes. Over two regimes of the parameters, the system has only one stable state: dry or wet; over a certain regime with small minimum PE ( $PE_{\min}$ ) and properly large coupling strength ( $\alpha$ ) relative to the recycling ratio ( $\rho$ ), the system has two stable states: dry and wet. Only stable equilibriums can exist in nature. When there is only

Table 1. Parameter Values Used in the Model

Parameter	Value	Unit	Source
$E_p$	5	mm/day	Mintz and Walker [1993]
$T$	360	days	
$S_{wp}$	0.3		Dickinson <i>et al.</i> [1993]
$S_{fc}$	0.74		Dingman [2002]
$c$	2		Lowry [1959]
$k_b$	0.82		Campbell and Norman [1998]
$D\phi$	1000	mm	Entekhabi <i>et al.</i> [1992]
$K_s$	1000	mm/day	Dickinson <i>et al.</i> [1993]
$B$	4		Dickinson <i>et al.</i> [1993]
$k_p$	0.75		Zeng <i>et al.</i> [1999]
$\tau_l$	10	days	
$\tau_w$	4	years	
$q$	0.25		Rodriguez-Iturbe <i>et al.</i> [1999b]
$PE_{\min}$	0.2		
$\alpha$	0.4		
$m$	0.5		
$\bar{\rho}$	0.3		Brubaker <i>et al.</i> [1993]
$\sigma_\rho$	0.1		Brubaker <i>et al.</i> [1993]

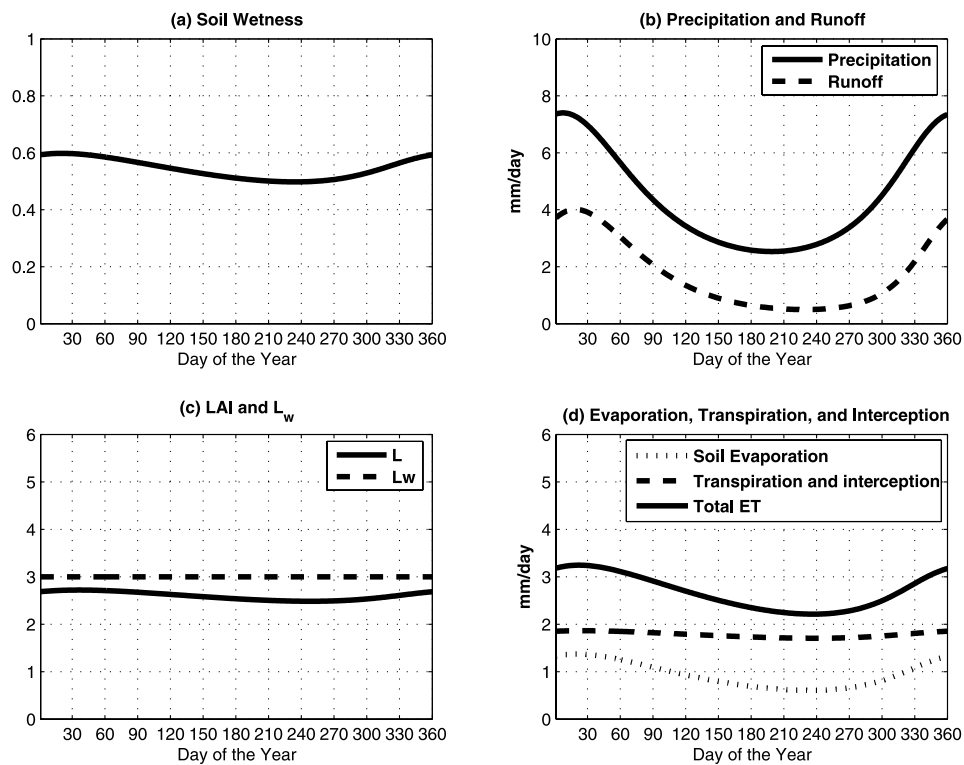


**Figure 2.** Model-simulated seasonal cycles of some variables at no external forcing.  $L_w$  is fixed at 3.

one stable equilibrium, the equilibrium state is not determined by the initial conditions; when there are two stable equilibriums, different initial conditions can reach totally different equilibrium states, but they can converge to an intermediate state with enough external forcing [Zeng and Neelin, 2000; D'Odorico et al., 2005]. The effect of the external forcing is determined by its strength and frequency; our results show that strong low-frequency forcing has the most significant effect (not shown). Moreover, catastrophic climate shift [Scheffer et al., 2001] can happen when the change of parameter values makes the climate move from one regime to another. Some results of the impacts of initial land covers and external forcings on the equilibrium states from a more complex model are given by Wang [2004]. Our results are similar and will not be presented here.

## 4. Experiments and Results

### 4.1. Experimental Design

[20] In order to study the land-atmosphere interaction for different land covers and at different external forcings, we performed a series of experiments. As monthly to seasonal climate variability is the focus of this paper, we assume that there is no large vegetation type transition and the  $L_w$  values are fixed for each land cover. In the first experiment (Exp1), the  $L_w$  values are fixed at 0.5, 2, 3.5, and 5 to represent four different land covers from sparse to dense: desert, grassland, tree-grass mixture and forest. For each land cover, three 50-year runs are performed with external forcing strength  $\sigma = 2, 0.5,$  and  $0.1,$  respectively. The second experiment (Exp2) is the same as the first one except that the average seasonal cycles of LAI from the last 40 years of first experiment are used, so there is no interannual variability in LAI, but other variables are still calculated. In the third experiment (Exp3),

average seasonal cycles of both LAI and soil wetness from the first experiment are used, so there is no interannual variability in either LAI or soil wetness. The output of the last 40 years of each run is used for analysis. Hence the difference between Exp1 and Exp2 can be regarded as showing the influence of interactive vegetation, and the

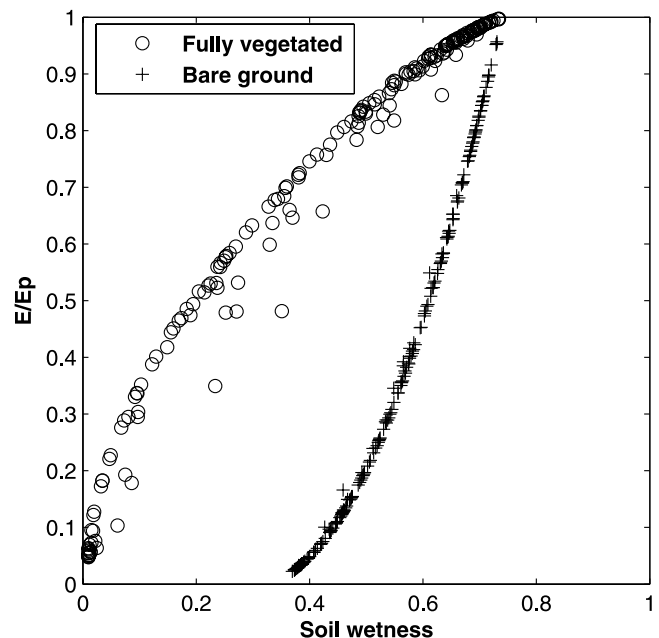


**Figure 3.** ET normalized by its potential value as a function of soil wetness for bare ( $L_w = 0.01$ ) and fully vegetated ( $L_w = 6$ ) land. Monthly average values are shown.

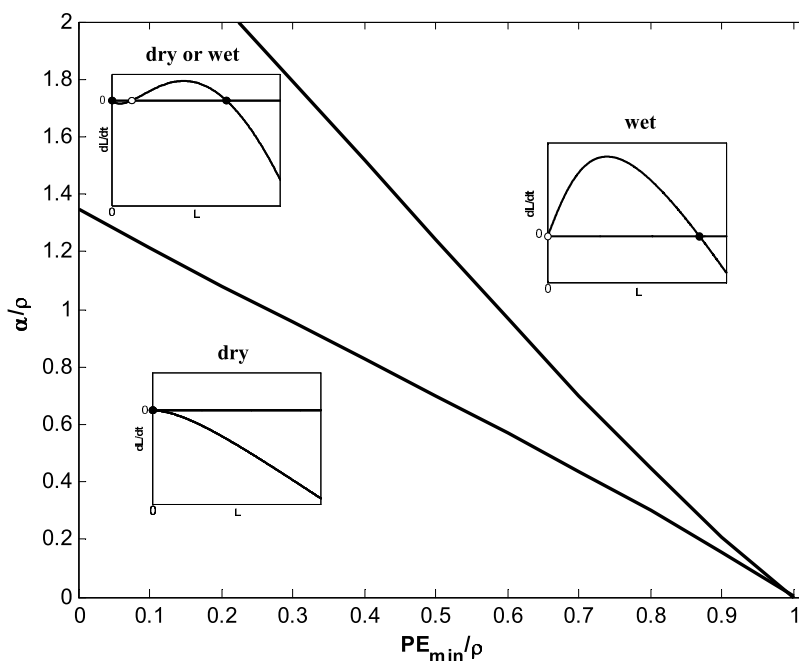


**Figure 4.** Equilibrium states of LAI ( $L$ ) in the parameter regime of  $PE_{\min}/\rho$  and  $\alpha/\rho$ . Here  $\rho$  has no seasonal cycle. The inserts show the  $dL/dt - L$  relation. The solid circles in the inserts are stable equilibrium states and open circles are unstable equilibrium states. Other hydroclimatological variables such as maximum LAI ( $L_w$ ), soil wetness ( $S$ ), and precipitation ( $P$ ) have similar multiequilibrium states as LAI.

difference between Exp2 and Exp3 can be regarded as showing the influence of interactive soil wetness.

#### 4.2. Data Analysis Methods

[21] Although this is a simple model, it includes substantial nonlinearity and complex interactions. Statistical methods are used to analyze its output variables. The temporal variabilities of the variables are estimated by their autocorrelation. If we assume that the time series of the variable are similar to a red noise of first-order Markov process [e.g., *Delworth and Manabe, 1988*], the autocorrelation value can be calculated as [*Daniel, 1995*]

$$r(t) = \exp(-t/\tau), \quad (18)$$

where  $\tau$  is the decay timescale, and the autocorrelation  $r$  will reach the e-folding value when  $t = \tau$ . In this study, we use the lag-one-month autocorrelation to calculate  $\tau$ . The  $\tau$  value provides a single parameter measure of the memory or persistence of the variables, and can also be used as a measure of predictability. In this paper, the memory, persistence, and predictability all denote the  $\tau$  values. Note that as the autocorrelation of the hydroclimatological variables in this study decay to insignificant values in 1 year, the  $\tau$  value is only a measure of monthly to seasonal variability.

[22] As the time series of external forcing contains variations of all kinds of frequencies, the wavelet transform [*Torrence and Compo, 1998; Grinsted et al., 2004*] is used to analyze it at local time and frequency and its influence on the land-atmosphere interaction. Most traditional methods that examine periodicities in the frequency domain, such as

Fourier analysis, have implicitly assumed that the time series are stationary in time and give an average power spectrum for the whole time series. However, most geophysical time series are nonstationary. Wavelet transforms can expand time series into time-frequency space and therefore find localized variability.

[23] In order to examine the coupling between soil wetness and precipitation, the cross-wavelet coherency analysis [*Torrence and Compo, 1998; Torrence and Webster, 1999; Grinsted et al., 2004*] is used. The cross-wavelet coherency finds regions in time frequency space where the two time series covary (in phase or out of phase) but do not necessarily have high power. It is defined as the absolute value squared of the smoothed cross-wavelet spectrum normalized by the smoothed wavelet power spectra. This definition resembles that of the squared correlation coefficient, and it is useful to think of the wavelet coherency as a localized correlation coefficient in time-frequency space. The unique feature of this method is that it measures the local values of both coherency and phase lag of the two time series continuously through time. This feature is overlooked by many other statistical methods, for example, correlation, lagged correlation, and cross spectrum analysis, which describe an average relationship of two time series over a specified time.

#### 4.3. Results

[24] The  $\tau$  values for the soil wetness and precipitation anomaly (seasonal cycle removed) time series from the three experiments are shown in Figure 5. Generally, soil wetness has larger  $\tau$  values than precipitation, and their  $\tau$  values are larger than that of the noise in both Exp1 and Exp2

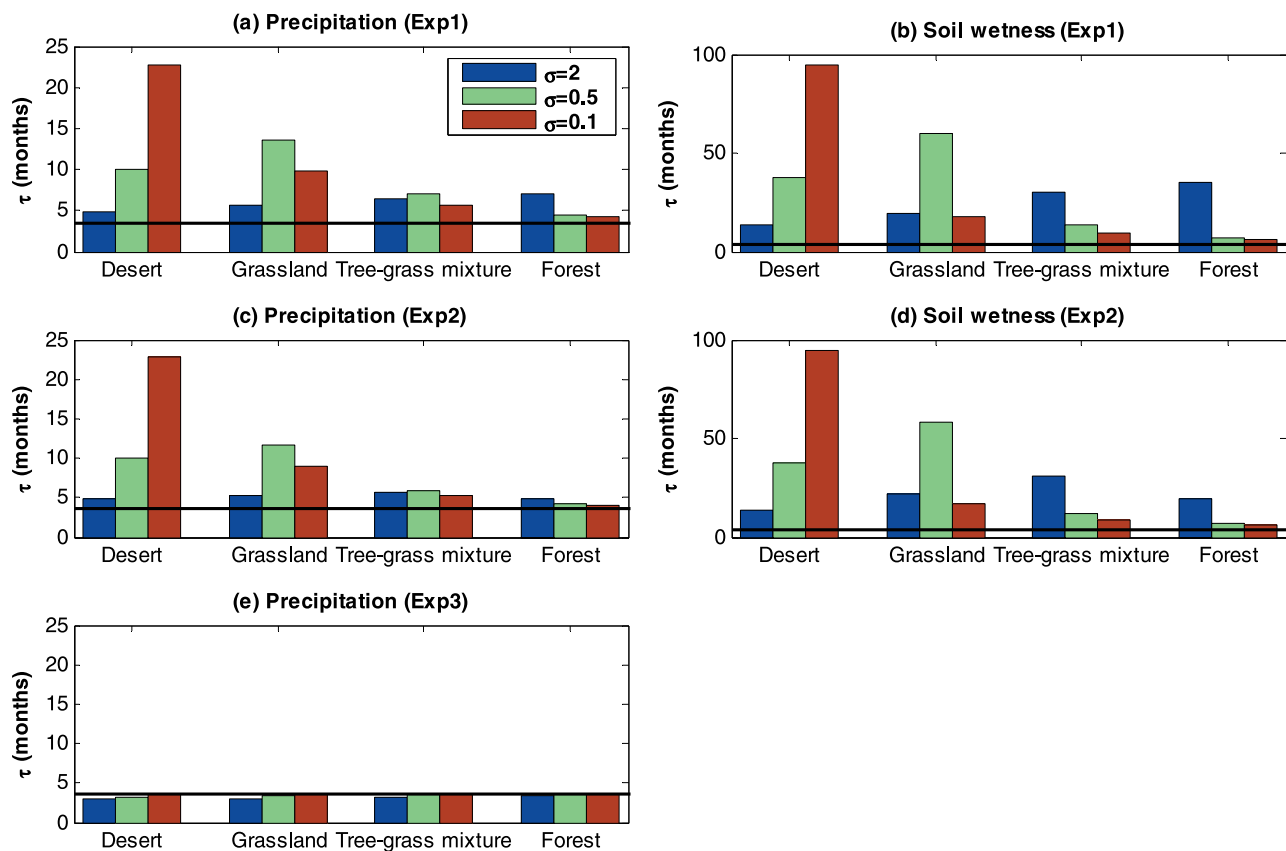


**Figure 5.** Decay timescale  $\tau$  of monthly soil wetness and precipitation anomaly for different land covers and at different forcing strengths. (a, b) Exp1. (c, d) Exp2. (e) Exp3. The horizontal black line is the  $\tau$  value of the external forcing. All autocorrelations used to calculate  $\tau$  values are above the 99% significant level.

(Figures 5a, 5b, 5c, and 5d), which demonstrates the memory of land and its ability to enhance climate predictability. Without the memory from land (both vegetation and soil moisture), the  $\tau$  values for precipitation in Exp3 are close to the noise (Figure 5e). Next, we will compare the results from different land covers and different experiments. Let us look at the results of Exp1 first (Figures 5a and 5b). It is evident that when the external forcing is strong ( $\sigma = 2$ ), the  $\tau$  values at the forest are the largest; with the weakening of the external forcing ( $\sigma = 0.5, 0.1$ ), the peak  $\tau$  values move to the grassland and then to the desert. Thus the peak  $\tau$  values tend to move from dense to sparse vegetation covers with the weakening of the external forcing. That is, a dense vegetation cover, with its large resilience, will take a long time to recover from a dry or wet anomaly caused by a strong external forcing, while if the external forcing is weak, the internal interactions in the land-atmosphere system will induce some high-frequency variability relative to the average state, although in smaller amplitude than that from a stronger forcing, and decrease the climate persistence. On the contrary, a sparse vegetation cover has little memory and is more responsive to a strong forcing; hence the memory and  $\tau$  values will be smaller with a strong forcing. In Exp2, after we fix the LAI to the seasonal climatologies, the  $\tau$  values for a certain forcing decrease over the vegetated land and have little change over desert (Figures 5c and 5d). The reason is that climate-vegetation

interaction can damp the high-frequency climate variability and increase the climate persistence [Zeng *et al.*, 1999; Wang and Eltahir, 2000c].

[25] Of the three forcing strengths for the precipitation ( $\sigma = 2, 0.5$ , and  $0.1$ ),  $\sigma = 0.5$  is most realistic (as can be judged from the signal-to-noise ratio), so its  $\tau$  values as measuring precipitation predictability are most close to the current climate and can be compared with other studies. If we assume that the contributions of interactive soil wetness and interactive vegetation to the  $\tau$  values linearly add, we can analyze their respective contributions from the  $\tau$  value differences of the three experiments (Figure 6). It is found that soil wetness contributes more to the predictability over all the land covers, and that the contribution of interactive vegetation is much smaller over sparse vegetation covers and comparable only at dense vegetation covers; the percentage of contribution from interactive vegetation increases with vegetation density. Moreover, the contribution of soil wetness to the predictability is largest at the grassland, which is consistent with previous GCM results that soil moisture contributes most to precipitation predictability in transitional zones between dry and humid climates [Koster *et al.*, 2000, 2004]. The contribution of interactive vegetation is largest over the tree-grass mixture and grassland and is reduced over forest by the large resilience and saturation effects. However, the maximum contributions of soil wetness and interactive vegetation (at grassland in Figure 6) will move to a denser (sparser)

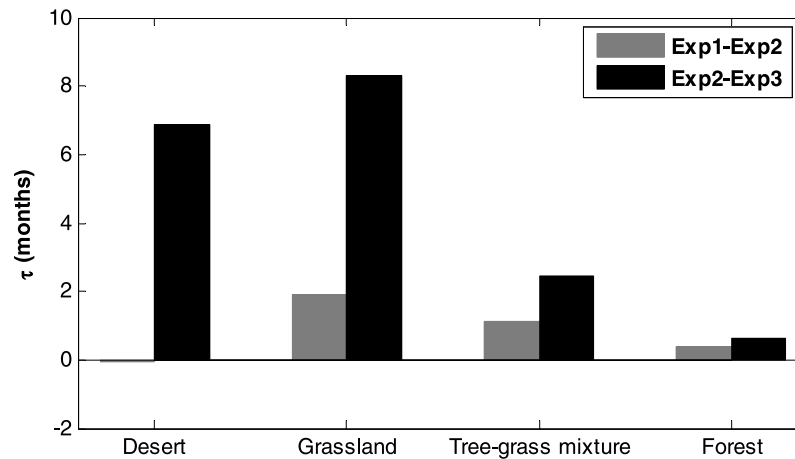


**Figure 6.** The  $\tau$  value difference of precipitation at forcing strength  $\sigma = 0.5$  for different land covers. Bright bars are for Exp1–Exp2, which is the contribution of interactive vegetation to the precipitation predictability; dark bars are for Exp2–Exp3, which is the contribution of soil wetness to the precipitation predictability.

vegetation cover with the strengthening (weakening) of external forcing (not shown). This moving indicates that the “hot spots” of land-atmosphere interaction suggested by *Koster et al.* [2004] may move in a future climate change.

[26] The cross-wavelet coherency between soil wetness and precipitation for Exp1 and Exp2 at forcing strength  $\sigma = 0.5$  is shown in Figure 7. In general, there is more coherency at low frequencies than at high frequencies because the soil moisture and precipitation correlates better at longer timescales. The vegetated lands have less low-frequency coherency than desert for both experiments because of vegetation shading, interception and soil-vegetation-atmosphere interaction. With the vegetation fixed at seasonal climatologies, Exp2 shows almost the same coherency pattern as Exp1 except that the coherency is weakened in some low-frequency regime owing to lack of vegetation interaction (Figure 7f). This weakening illustrates that the interactive vegetation may enhance the low-frequency soil wetness-precipitation coherency. In addition, as talked about above, the influence of interactive vegetation depends on the strength of external forcing, and the maximum influence (Figure 7f) may move to denser vegetation with the strengthening of the forcing (not shown). Owing to the complex nonlinear interactions in the model, the coherency patterns vary nonlinearly with the forcing strength (not shown), but several weak coherency centers exist regardless of the forcing strengths, such as the weak centers around (50, 8), (200, 0–4), (200, 16–32), (380, 0–4), and (420, 0–4) (Figure 7).

[27] In order to further investigate the relationship between the coherency and external forcing, we compare the coherency pattern with the wavelet power spectrum of the forcing time series ( $F$ ) in the same time-frequency domain (Figures 7 and 8). It is found that the weak coherency centers in Figures 7a and 7e (as listed above) correspond very well to the weak power centers in Figure 8 for both high and low frequencies. We only compare the coherency centers appear at desert because they may be amplified or slightly moved by stronger vegetation influence at other

land covers. Evidently, this good correspondence indicates that much of the large coherency between soil wetness and precipitation is due to the strong external forcing, and during periods of weak forcing the coherency will be small. This corresponds to a “threshold effect” as suggested by *Oglesby et al.* [2002]: A strong external forcing can induce a large soil wetness anomaly, which can lead to a strong feedback that make precipitation and soil wetness vary in the same direction; while if the external forcing is weak, the precipitation and soil wetness anomalies will be small, and the coherency will be weakened by the variability of atmospheric and land processes.

[28] As the parameterization of precipitation is a very uncertain part of our model, and a slight change of the parameter values may, as mentioned in section 3, lead to completely different equilibrium states, some experiments are performed with a little different  $PE_{\min}$  and  $\alpha$  values, different formation of equation (16), and different noise. No qualitative change is found in the results except that the positions of peak  $\tau$  values in Figure 5 may move with climate change.

## 5. Conclusions and Discussion

[29] This study develops a simple model of warm climate land-atmosphere interaction with interactive land components: soil wetness and vegetation. Because of its simplicity, such a model is useful for many applications; for example, it can be easily integrated for a long time to estimate the trend of climate variation, it can clearly separate variability from different sources and analyze their individual influence on climate variability, and different climate conditions can be easily represented by changing a few model parameters. However, its simplicity may lead to difficulties; it has no variability from energy balance or related processes, no boundary layer processes, and no atmospheric dynamics. Although these limitations may reduce the applicability of this model, it is especially suitable for study of climate variability on seasonal to decadal timescales and can provide some guidance for GCM study.

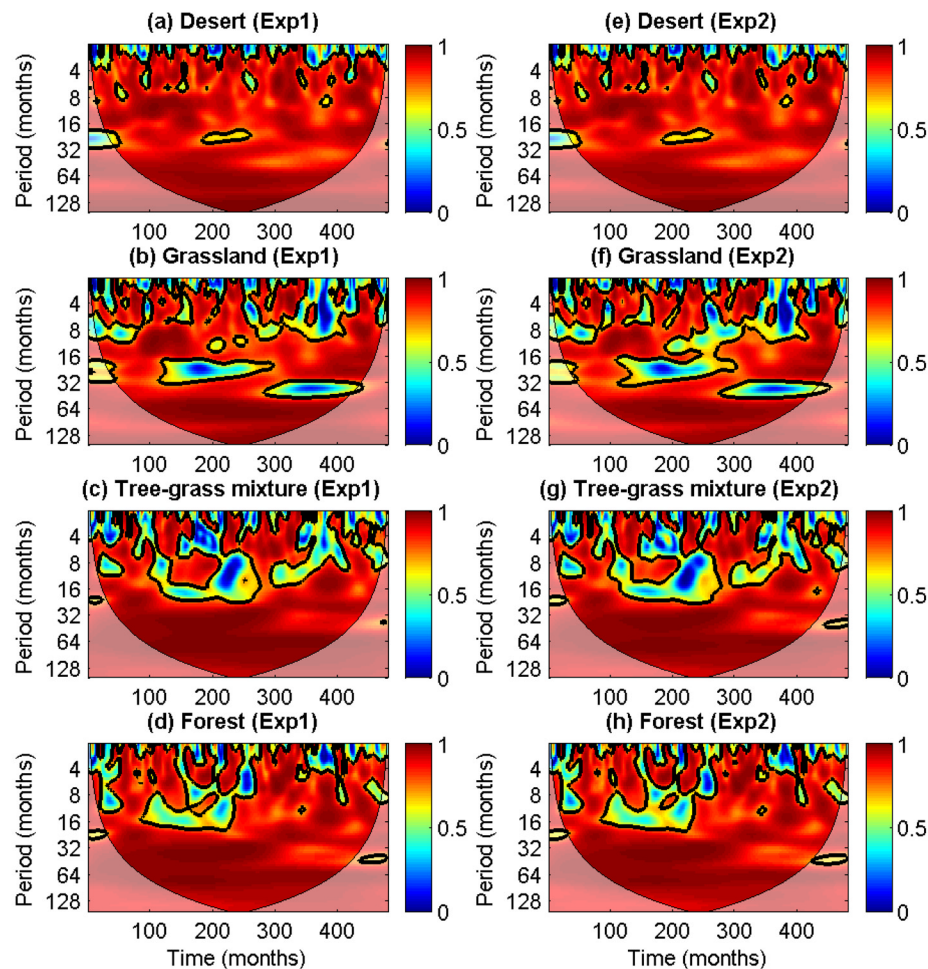


**Figure 7.** Cross-wavelet coherency between soil wetness and precipitation anomalies for different land covers. Forcing strength  $\sigma = 0.5$ . (a, b, c, d) Exp1. (e, f, g, h) Exp2. The thick black contour is 5% significance level against red noise, and the cone of influence where edge effects might distort the picture is shown as a lighter shade. The phase information is not shown in this figure. Generally, precipitation leads soil wetness about one-eighth period at periods less than 1 year and is in phase with soil wetness at periods larger than 1 year.

[30] The model is used to study the role of land surface processes in climate variability over different land covers and at different external forcings. The major findings and their implications for the current model studies on warm climate land-atmosphere interaction and climate prediction are as follows.

[31] 1. The decay timescales of soil wetness and precipitation maximize at sparser (denser) vegetation covers with the weakening (strengthening) of external forcing. Hence both the strength of external variabilities and the regional land cover influence the soil moisture and precipitation persistence. In a model, these external variabilities can come from natural regional climate variability or incorrect model internal dynamics. These incorrect variabilities in the model may act on the simulated soil moisture and precipitation persistence and even transfer to other component in the climate system [e.g., Wang and Eltahir, 2000b]. Therefore accurate simulation of climate variability besides mean climate is an urgent task facing model developers.

[32] 2. The persistence of soil wetness and precipitation is larger with interactive vegetation, if it is dense, and changes little, if vegetation is sparse. Thus fixing vegetation in a model may underestimate the soil moisture memory and precipitation predictability for densely vegetated warm regions. Interactive vegetation in these regions is necessary if a good estimate of soil moisture memory and precipitation predictability is desired.

[33] 3. Interactive vegetation can enhance the low-frequency coherency between soil wetness and precipitation at some land covers (depending on the forcing), but its influence on high-frequency coherency is small. Thus fixed seasonal vegetation will not have much influence on the soil wetness–precipitation relationship at monthly to seasonal timescales. It also appears that interactive soil moisture is more important than interactive vegetation for precipitation variation at these timescales. This is due to the different ways soil moisture and vegetation interacts with the atmosphere. Observational data also show that the local vegetation feedback has little influence on precipitation at monthly

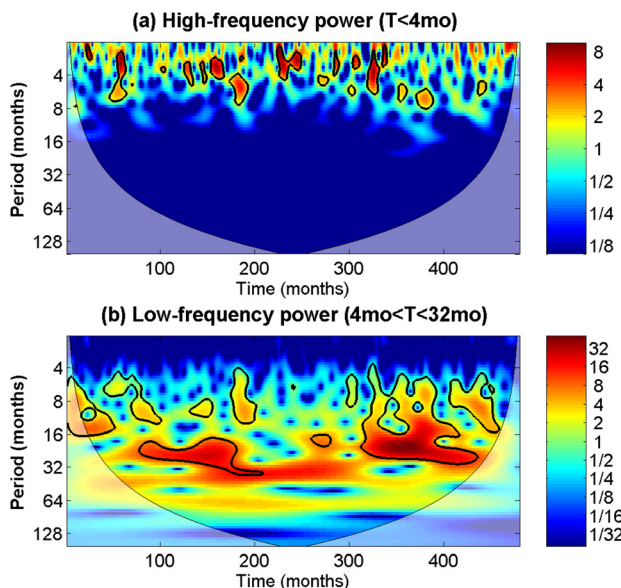


**Figure 8.** Continuous wavelet power spectrum of the external forcing. (a) High-frequency power (period  $T < 4$  months). (b) Low-frequency power ( $4 \text{ months} < T < 32$  months). The thick black contour is 5% significance level against red noise, and the cone of influence where edge effects might distort the picture is shown as a lighter shade.

to seasonal timescales and the influence is larger at a longer timescale [Liu *et al.*, 2006] when the vegetation succession plays an important role [Zeng *et al.*, 1999].

[34] 4. A strong external forcing can induce a large soil wetness anomaly and a large coherency between soil wetness and precipitation, while such coherency may be weak if the external forcing is weak. As the feedback between soil moisture and precipitation can induce a lagged relationship between them [Eltahir, 1998; D'Odorico and Porporato, 2004], soil moisture has been used as an initial condition to predict precipitation in some studies [e.g., Fennessy and Shukla, 1999; Douville and Chauvin, 2000]. Our study on their coherency shows that their relationship depends on the

strength of external forcing; a strong external forcing at a certain time and frequency can induce a strong coherency (simultaneous or lagged relationship) between soil moisture and precipitation at a corresponding time and frequency. As external forcing is usually nonstationary, their relationship and coherency also exhibit an on-and-off feature.

[35] In this study, the influence of local land processes on precipitation predictability is divided into the contribution from soil wetness and the contribution from interactive vegetation. This influence can also be divided into the contribution from ET and the contribution from PE (equation (15)). In order to study their relative importance, two additional experiments are performed with ET or PE fixed at seasonal climatologies of Exp1 to neglect their interannual variabilities. They are denoted Exp4 and Exp5, respectively. By comparing the  $\tau$  value difference for precipitation between these two experiments and fully interactive Exp1, we can obtain the contribution of ET and PE to the precipitation predictability, respectively. Figure 9 shows that both ET and PE can contribute to the precipitation predictability, but that the contribution of ET is much larger. The reason may be that there is no seasonal temperature variation in the warm climate we assumed. As PE is mainly controlled by the monthly temperature, its changes will be small, while ET, which is mainly controlled by surface soil wetness and vegetation, will have a relatively large change. Thus fixing ET at seasonal climatologies will decrease its control on precipitation and the precipitation variability will mainly come from external forcing with little predictability, while fixing PE at seasonal climatologies has a relative small influence on the precipitation predictability. In this sense, ET is more important than PE in the warm climate seasonal precipitation prediction.

[36] A major simplification of the model is its neglect of atmospheric dynamics and ocean interaction. Although the red component of the added forcing is similar to the persistence of the atmosphere and ocean, the linear precipitation parameterization neglects the possible scale interactions in the climate system, such as the interactions between tropical convection, Madden-Julian oscillation, and ENSO. This neglect may be the reason the weak coherency centers between soil wetness and precipitation corresponds so well

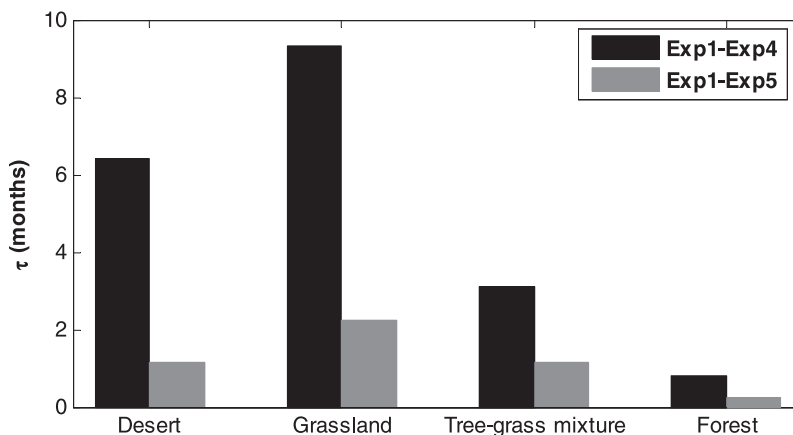


**Figure 9.** Same as Figure 6 except dark bars are for Exp1–Exp4, which is the contribution of ET to the precipitation predictability; bright bars are for Exp1–Exp5, which is the contribution of PE to the predictability.

to the weak wavelet power centers of external forcing in the time-frequency domain. Hence these results need to be examined by coupled nonlinear models.

[37] This model provides a framework for revision or further development as needed. The precipitation and vegetation parameterizations of the model are designed for warm climate with convective precipitation. With more feedbacks from temperature, radiation, and chaotic atmospheric dynamics, the land-atmosphere interaction processes in cooler climate will be more complex, but their study may be guided by the results attained here.

[38] **Acknowledgments.** This work was supported by NSF grant ATM-03433485. Cross-wavelet and wavelet coherence software were provided by A. Grinsted. The authors are grateful to the suggestions and comments from G. Wang, W. Wu, Q. Liu, H. Chen, J. Zhang, W. Shem, and two anonymous reviewers that substantially improved the manuscript.

## References

- Brovkin, V., S. Levis, M. F. Loutre, M. Crucifix, M. Claussen, A. Ganopolski, C. Kubatzki, and V. Petoukhov (2003), Stability analysis of the climate-vegetation system in northern high latitudes, *Clim. Change*, *57*, 119–138.
- Brubaker, K. L., D. Entekhabi, and P. S. Eagleson (1993), Estimation of continental precipitation recycling, *J. Clim.*, *6*, 1077–1089.
- Campbell, G. S., and J. M. Norman (1998), *An Introduction to Environmental Biophysics*, 2nd ed., 286 pp., Springer, New York.
- Charney, J. G. (1975), Dynamics of deserts and drought in the Sahel, *Q. J. R. Meteorol. Soc.*, *101*, 193–202.
- Clapp, R. B., and G. M. Hornberger (1978), Empirical equations for some soil hydraulic properties, *Water Resour. Res.*, *14*, 601–604.
- Clark, D. B., Y. Xue, R. J. Harding, and P. J. Valdes (2001), Modeling the impact of land surface degradation on the climate of tropical north Africa, *J. Clim.*, *14*, 1809–1822.
- Cramer, W., et al. (2001), Global response of terrestrial ecosystem structure and function to CO<sub>2</sub> and climate change: Results from six dynamic global vegetation models, *Global Change Biol.*, *7*, 357–373.
- Daniel, S. W. (1995), *Statistical Methods in the Atmospheric Sciences*, 467 pp., Elsevier, New York.
- Delire, C., J. A. Foley, and S. Thompson (2004), Long-term variability in a coupled atmosphere-biosphere model, *J. Clim.*, *17*, 3947–3959.
- Delworth, T., and S. Manabe (1988), The influence of potential evaporation on the variabilities of simulated soil wetness and climate, *J. Clim.*, *1*, 523–547.
- Delworth, T., and S. Manabe (1989), The influence of soil wetness on near-surface atmospheric variability, *J. Clim.*, *2*, 1447–1462.
- Dickinson, R. E., and P. Kennedy (1992), Impact on regional climate of Amazonian deforestation, *Geophys. Res. Lett.*, *19*, 1947–1950.
- Dickinson, R. E., and A. Henderson-Sellers (1988), Modelling tropical deforestation: A study of GCM land-surface parametrizations, *Q. J. R. Meteorol. Soc.*, *114*, 439–462.
- Dickinson, R. E., A. Henderson-Sellers, and P. J. Kennedy (1993), Biosphere Atmosphere Transfer Scheme (BATS) version 1e as coupled to the NCAR Community Climate Model, *NCAR Tech. Note NCAR/TN-387+STR*, 72 pp., Natl. Cent. for Atmos. Res., Boulder, Colo.
- Dingman, S. L. (2002), *Physical Hydrology*, 2nd ed., 646 pp., Prentice-Hall, Upper Saddle River, N. J.
- D'Odorico, P., and A. Porporato (2004), Preferential states in soil moisture and climate dynamics, *Proc. Natl. Acad. Sci. U. S. A.*, *101*, 8848–8851.
- D'Odorico, P., F. Laio, and L. Ridolfi (2005), Noise-induced stability in dryland plant ecosystems, *Proc. Natl. Acad. Sci. U. S. A.*, *102*, 10,819–10,822.
- Douville, H., and F. Chauvin (2000), Relevance of soil moisture for seasonal climate predictions: A preliminary study, *Clim. Dyn.*, *16*, 719–736.
- Eltahir, E. A. B. (1996), The role of vegetation in sustaining large-scale atmospheric circulations in the tropics, *J. Geophys. Res.*, *101*, 4255–4267.
- Eltahir, E. A. B. (1998), A soil moisture–rainfall feedback mechanism: 1. Theory and observations, *Water Resour. Res.*, *34*, 765–776.
- Eltahir, E. A. B., and R. L. Bras (1996), Precipitation recycling, *Rev. Geophys.*, *34*, 367–378.
- Entekhabi, D., I. Rodriguez-Iturbe, and R. L. Bras (1992), Variability in large-scale water balance with land surface-atmosphere interaction, *J. Clim.*, *5*, 798–813.
- Fennessy, M. J., and J. Shukla (1999), Impact of initial soil wetness on seasonal atmospheric prediction, *J. Clim.*, *12*, 3167–3180.
- Foley, J. A., I. C. Prentice, N. Ramankutty, S. Levis, D. Pollard, S. Sitch, and A. Haxeltine (1996), An integrated biosphere model of land surface processes, terrestrial carbon balance, and vegetation dynamics, *Global Biogeochem. Cycles*, *10*, 603–628.
- Fu, C. B. (2003), Potential impacts of human-induced land cover change on East Asia monsoon, *Global Planet. Change*, *37*, 219–229.
- Grinsted, A., J. Moore, and S. Jevrejeva (2004), Application of the cross wavelet transform and wavelet coherence to geophysical time series, *Nonlinear Proc. Geophys.*, *11*, 561–566.
- Henderson-Sellers, A., A. J. Pitman, P. K. Love, P. Irannejad, and T. Chen (1995), The Project for Intercomparison of Land Surface Parameterisation Schemes (PILPS) phases 2 and 3, *Bull. Am. Meteorol. Soc.*, *76*, 489–503.
- Koster, R. D., and M. J. Suarez (1995), Relative contributions of land and ocean processes to precipitation variability, *J. Geophys. Res.*, *100*, 13,775–13,790.
- Koster, R. D., M. J. Suarez, and M. Heiser (2000), Variance and predictability of precipitation at seasonal-to-interannual timescales, *J. Hydrometeorol.*, *1*, 26–46.
- Koster, R. D., et al. (2004), Regions of strong coupling between soil moisture and precipitation, *Science*, *305*, 1138–1140.
- Lean, J., and D. A. Warrilow (1989), Simulation of the regional climatic impact of Amazon deforestation, *Nature*, *342*, 411–413.
- Levis, S., and G. Bonan (2004), Simulating springtime temperature patterns in the Community Atmosphere Model coupled to the Community Land Model using prognostic leaf area, *J. Clim.*, *17*, 4531–4540.
- Liu, S. K., S. D. Liu, Z. T. Fu, and S. Lan (2005), A nonlinear coupled soil moisture-vegetation model, *Adv. Atmos. Sci.*, *22*, 337–343.
- Liu, Y., and R. Avissar (1999), A study of persistence in the land-atmosphere system with a fourth-order analytical model, *J. Clim.*, *12*, 2154–2168.
- Liu, Z., M. Notaro, J. Kutzbach, and N. Liu (2006), Assessing global vegetation–climate feedbacks from observation, *J. Clim.*, *19*, 787–814.
- Lofgren, B. M. (1995), Sensitivity of land–ocean circulations, precipitation, and soil moisture to perturbed land surface albedo, *J. Clim.*, *8*, 2521–2542.
- Lowry, W. P. (1959), The falling rate phase of evaporative soil moisture loss: A critical evaluation, *Bull. Am. Meteorol. Soc.*, *40*, 605.
- Mintz, Y., and G. K. Walker (1993), Global fields of soil moisture and land surface evapotranspiration derived from observed precipitation and surface air temperature, *J. Appl. Meteorol.*, *32*, 1305–1334.
- Oglesby, R. J., S. Marshall, D. J. Erickson, J. O. Roads, and F. R. Robertson (2002), Thresholds in atmosphere–soil moisture interactions: Results from climate model studies, *J. Geophys. Res.*, *107*(D14), 4224, doi:10.1029/2001JD001045.
- Pitman, A. J. (2003), The evolution of, and revolution in, land surface schemes designed for climate models, *Int. J. Climatol.*, *23*, 479–510.
- Rodriguez-Iturbe, I., D. Entekhabi, and R. F. Bras (1991), Nonlinear dynamics of soil moisture at climate scales: 1. Stochastic analysis, *Water Resour. Res.*, *27*, 1899–1906.
- Rodriguez-Iturbe, I., P. D'Odorico, A. Porporato, and L. Ridolfi (1999a), On the spatial and temporal links between vegetation, climate and soil moisture, *Water Resour. Res.*, *35*, 3709–3722.
- Rodriguez-Iturbe, I., P. D'Odorico, A. Porporato, and L. Ridolfi (1999b), Tree-grass coexistence in savannas: The role of spatial dynamics and climate fluctuations, *Geophys. Res. Lett.*, *26*, 247–250.
- Scanlon, B. R., D. G. Levitt, R. C. Reedy, K. E. Keese, and M. J. Sully (2005), Ecological controls on water-cycle response to climate variability in deserts, *Proc. Natl. Acad. Sci. U. S. A.*, *102*, 6033–6038.
- Scheffer, M., S. Carpenter, J. A. Foley, C. Folke, and B. Walker (2001), Catastrophic shifts in ecosystems, *Nature*, *413*, 591–596.
- Taylor, C. M., E. F. Lambin, N. Stephenne, R. J. Harding, and R. L. H. Essery (2002), The influence of land use change on climate in the Sahel, *J. Clim.*, *15*, 3615–3629.
- Torrence, C., and G. P. Compo (1998), A practical guide to wavelet analysis, *Bull. Am. Meteorol. Soc.*, *79*, 61–78.
- Torrence, C., and P. Webster (1999), Interdecadal changes in the ENSO-monsoon system, *J. Clim.*, *12*, 2679–2690.
- Trenberth, K. E. (1999), Atmospheric moisture recycling: Role of advection and local evaporation, *J. Clim.*, *12*, 1368–1381.
- Voldoire, A., and J. F. Royer (2004), Tropical deforestation and climate variability, *Clim. Dyn.*, *22*, 857–874.
- Wang, G. (2004), A conceptual modeling study on biosphere-atmosphere interactions and its implications for physically based climate modeling, *J. Clim.*, *17*, 2572–2583.
- Wang, G., and E. A. B. Eltahir (2000a), Ecosystem dynamics and the Sahel drought, *Geophys. Res. Lett.*, *27*, 95–98.
- Wang, G., and E. A. B. Eltahir (2000b), Modeling the biosphere-atmosphere system: The impact of the sub-grid variability in rainfall interception, *J. Clim.*, *13*, 2887–2899.

- Wang, G., and E. A. B. Eltahir (2000c), The role of ecosystem dynamics in enhancing the low-frequency variability of the Sahel rainfall, *Water Resour. Res.*, *36*, 1013–1021.
- Wang, G., E. A. B. Eltahir, J. A. Foley, D. Pollard, and S. Levis (2004), Decadal variability of rainfall in the Sahel: Results from the coupled GENESIS-IBIS atmosphere-biosphere model, *Clim. Dyn.*, *22*, 625–637, doi:10.1007/s00382-004-0411-3.
- Xue, Y. (1996), The Impact of desertification in the Mongolian and the Inner Mongolian grassland on the regional climate, *J. Clim.*, *9*, 2173–2189.
- Xue, Y., and J. Shukla (1993), The influence of land surface properties on Sahel climate: Part I. Desertification, *J. Clim.*, *6*, 2232–2245.
- Xue, Y., H.-M. H. Juang, W. Li, S. Prince, R. DeFries, Y. Jiao, and R. Vasic (2004), Role of land surface processes in monsoon development: Part I. East Asia and West Africa, *J. Geophys. Res.*, *109*, D03105, doi:10.1029/2003JD003556.
- Zeng, N. (1998), Understanding climate sensitivity to tropical deforestation in a mechanistic model, *J. Clim.*, *11*, 1969–1975.
- Zeng, N., and J. D. Neelin (1999), A land-atmosphere interaction theory for the tropical deforestation problem, *J. Clim.*, *12*, 857–872.
- Zeng, N., and J. D. Neelin (2000), The role of vegetation-climate interaction and interannual variability in shaping the African savanna, *J. Clim.*, *13*, 2665–2670.
- Zeng, N., J. D. Neelin, K.-M. Lau, and C. J. Tucker (1999), Enhancement of interdecadal climate variability in the Sahel by vegetation interaction, *Science*, *286*, 1537–1540.
- Zeng, X., S. S. P. Shen, X. Zeng, and R. E. Dickinson (2004), Multiple equilibrium states and the abrupt transitions in a dynamical system of soil water interacting with vegetation, *Geophys. Res. Lett.*, *31*, L05501, doi:10.1029/2003GL018910.
- Zhang, X., M. A. Friedl, C. B. Schaaf, A. H. Strahler, and Z. Liu (2005), Monitoring the response of vegetation phenology to precipitation in Africa by coupling MODIS and TRMM instruments, *J. Geophys. Res.*, *110*, D12103, doi:10.1029/2004JD005263.
- Zheng, X., and E. A. B. Eltahir (1997), The response to deforestation and desertification in a model of West African monsoon, *Geophys. Res. Lett.*, *24*, 155–158.

---

R. E. Dickinson and J. Wei, School of Earth and Atmospheric Sciences, Georgia Institute of Technology, Atlanta, GA 30332-0340, USA. (robted@eas.gatech.edu; jwei@eas.gatech.edu)

N. Zeng, Department of Atmospheric and Oceanic Science and Earth System Science Interdisciplinary Center, University of Maryland at College Park, College Park, MD 20742, USA. (zeng@atmos.umd.edu)